BNL Brookhaven National Laboratory

RHIC Accelerator Physics Group

RHIC/AP/150

Beam Induced Electron Clouds at RHIC

Kirsten A. Drees

Abstract

The development of a beam induced electron cloud in the vacuum pipe of RHIC depends mainly on three parameters: the radius of the beam pipe, the secondary emission yield of the vacuum chamber material and the time gap between two consecutive bunches. A simple model estimates the mean survival probability of electrons in the beam pipe, the effective yield and the dissipated power in the chamber wall due to the electron cloud. Calculations are made taking into account two different operation schemes with 60 and 120 bunches respectively. No effect is expected for an operation with 60 bunches while the potential RHIC upgrade with 120 bunches runs the risk to produce an unacceptable heat load in the chamber wall.

March 13, 1998

1 Introduction

Electrons, produced by either ionization of residual gas or photo-emission in the chamber wall due to synchrotron radiation, are attracted and accelerated by the electrical field of the next passing bunch. Once these accelerated electrons hit the chamber wall they cause the emission of secondary electrons [1], which can eventually give rise to a continuous accumulation of electrons in the beam pipe. Once the cloud is established it is likely to cause beam instabilities and an enhanced gas desorption associated by a pressure increase. However, various conditions have to be met to build up a quasi-stationary electron cloud.

This electron cloud effect, first observed and reported in 1977 at the ISR [2] at CERN, was recently studied again by an LHC working group [3, 4, 5] and found to be critical for the upper limit of the linear power dissipation on the LHC beam screen. The alarming results of the LHC working group motivated a closer look at the possible impact of beam induced electron clouds on RHIC. At RHIC the contribution from synchrotron radiation (< 1 eV per turn for 250 GeV protons) to the primary electron production is negligible small, while it will be the dominant source at LHC. Electrons in the RHIC vacuum chamber arise from residual gas interactions with the beam. However, at RHIC the distance between two consecutive bunches is much larger than at the LHC allowing the secondary electrons to be absorbed before the next bunch arrives. This report provides results for an electron cloud development under conditions of the typical RHIC parameters.

2 The Model

A potential source of primary electrons at RHIC are interactions of the the beam with the residual gas. At RHIC both the cold vacuum and the warm vacuum consist mainly of H_2 ions, in the first case with balance being He and in the latter case with balance being CO [6]. Therefore the number of electrons N_e per cm in one turn is in good approximation equal to the number of H_2 and CO ions created by residual gas collisions with the beam:

$$\frac{dN_{ion}}{dl} = M \cdot N_b \cdot (\alpha_{H_2}\rho_{H_2}\sigma_{H_2} + \alpha_{co}\rho_{co}\sigma_{co}) = N_e/\mathrm{cm}, \tag{1}$$

where N_b is the number of particles per bunch, M is the number of bunches, ρ is the density of ions in the beam pipe corresponding to the quality of the vacuum and $\sigma_{H_2}, \sigma_{co}$ are the cross sections of the $Au - H_2$ and $Au - CO$ interaction respectively. α denotes the occurance of the molecule type within one turn depending on warm and cold sections. The ionization cross section which on the one hand is independent

from the charge and the mass of the ionizing particle on the other hand depends on the molecule of the residual gas and the velocity of the ionizing particle. It can be described by the following ("Bethe") formula [7]:

$$\sigma = 4\pi(\frac{\hbar}{mc})^2 \left[C_1^2\beta^2 \ln(\frac{\beta^2}{1-\beta^2}) - 1 \; + \; C_2\frac{1}{\beta^2} \right], \tag{2}$$

where C_1 and C_2 are constants with the particular values of:

molecule	C_1^2	C_2
H_2	0.5	8.1
co	3.7	35.1

Assuming a parabolically shaped bunch the electrical field $E(r)$ attracting these primary electrons is given by [8]:

$$E(r) = E_0 \left(2 - (\frac{r}{R})^2\right) \frac{r}{R}, \qquad \text{for } r \leq R\ , \tag{3}$$

$$E(r) = E_0 \frac{R}{r}, \qquad \text{for } r > R\ , \tag{4}$$

and

$$E_0 = \frac{I_{bunch}}{2\pi\epsilon_0\sigma_L R f_{rev}} \qquad . \tag{5}$$

Here are:

r	radial position
R	radius of charge distribution
f_{rev}	revolution frequency
I_{bunch}	bunch current
σ_L	bunch length

In a single kick approximation a stationary electron at a radial position r gains a certain amount of momentum Δp during the passage of a bunch:

$$\Delta p = e \cdot E(r) \cdot \frac{\sigma_L}{c} \qquad . \tag{6}$$

The momentum transfer corresponds to an energy gain of:

$$\Delta E = \frac{(\Delta p)^2}{2m_e} \qquad . \tag{7}$$

To develop an electron avalanche the accelerated electrons have to (i) cross the beam pipe at least once before the arrival of the next bunch and (ii) create secondary

electrons in the chamber wall. The first condition, which is easily accomplished for either RHIC operation mode, 60 and 120 bunches, can be expressed by [4]:

$$\frac{2 \cdot r_b \cdot m_e}{\Delta p} \leq t_{bb}, \tag{8}$$

where t_{bb} corresponds to the time between two successive bunches while r_b is the radius of the beam pipe. The second condition is met by any primary electrons which gained sufficient energy to produce more than 1 secondary electron when they hit the vacuum chamber wall. Two major ingredients influence the energy gain: the bunch intensity I_{bunch} and the RMS bunch length σ_L. In the single kick approximation according to equation 7, effects due to σ_L are neglected. However, in the case of long bunches electrons could oscillate several times inside the bunch potential leading to a mean energy gain which is shifted to smaller energies. Bunch intensities smaller than the nominal value, which are likely for the RHIC start up period, would result in a smaller value for the mean energy as well.

The secondary emission yield δ as a function of the angle of incidence Θ and the energy E of the initial electron can be parameterized in the following form [8]:

$$\delta(E,\Theta) = \delta_{max}\, 1.1\, \frac{1 - e^{-2.3\,(\frac{E}{E_{max}})^{4/3}}}{(\frac{E}{E_{max}})^{1/3}} \cdot e^{0.9\,(1-\cos(\Theta))} \quad . \tag{9}$$

The maximum value of this distribution, δ_{max}, and the energy where the maximum takes place, E_{max}, are both specific material constants, which are quoted in literature for various elements and compounds [9]. However, the quoted values for stainless

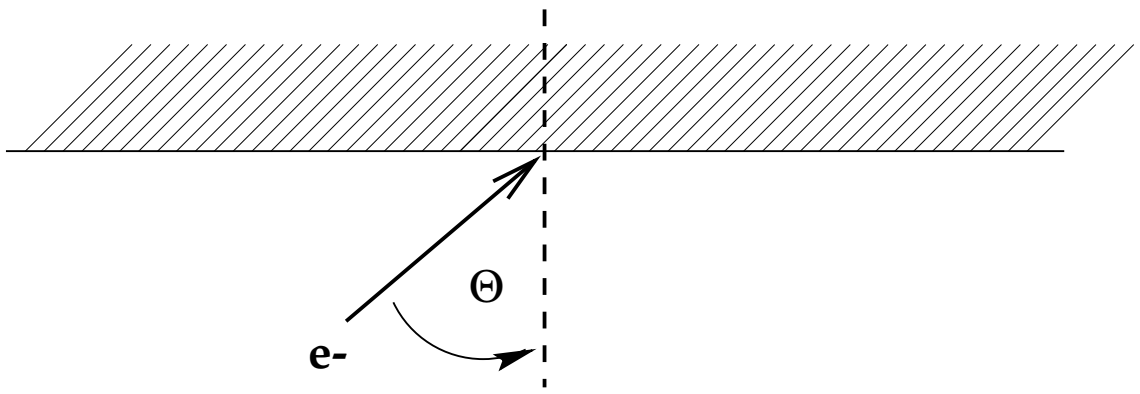

Figure 1: *Definition of angle of incidence in this report.*

steel differ by quite some amount from 1.2 [10] up to 2.0 [4]. Typically small values of δ_{max} are achieved for coated stainless steel, for conditioned surfaces or for a warm environment. According to the definition of Θ, which is outlined in figure 1,

perpendicular incidence corresponds to $\Theta = 0^o$. The secondary electron coefficient $\delta(E, \Theta)$ acquires a minimum for normal incidence and is increasing as a function of Θ up to an angle of $\Theta = 60^o$ at which the yield saturates [6].

3 Application to RHIC

Table 1 lists parameters which apply for RHIC and are used in the following calculations. Most parameters are taken from [11]. Note that $E_{max} = 300$ eV and the upper limit of δ_{max} are derived from measurements recently performed within LHC electron cloud studies [4]. $E_{max} = 500$ eV and the lower limit of δ_{max} are the values quoted in [10].

M	number of bunches	60/120
t_{bb}	bunch spacing	228.4/114.2 ns
r_b	beam pipe radius	0.0346 m
ρ	residual gas density at	
	4 K, 1 10^{-11} Torr (cold)	2 10^7 cm^{-3}
	300 K, 1 10^{-9} Torr (warm)	3 10^7 cm^{-3}
σ_{H_2}	cross section	2.3 10^{-19} cm^2
σ_{co}	cross section	1.2 10^{-18} cm^2
B	bending field	3.5 T
f_{rev}	revolution frequency	78.193 kHz
N_b	number of particles/bunch (gold)	1 $\cdot 10^9$
I_{bunch}	bunch current (gold)	1 mA
σ_L	RMS bunch length (gold start store)	0.11-0.17 m
R	radius of charge distribution ($\sigma_{h,v}$)	1.3-1.7 mm
δ_{max}	stainless steel	1.2 - 2.0
E_{max}	stainless steel	300 - 500 eV

Table 1: *Global RHIC parameters, values for operation with gold, and specific properties of stainless steel.*

The RMS bunch length used is 14 cm, which corresponds to a typical value at the beginning of a store with gold nuclei [12]. The residual gas in the cold bore is assumed to consist of H_2 only while it is assumed to be even distributed between H_2 and CO in the warm bore which corresponds to approximately 25% of the entire

ring. Based on the assumptions discussed above the number N_0 of primary electrons per bunch produced in one turn by a beam of 60 bunches can be evaluated according to equation 1:

$$\frac{dN_e}{dl} = 0.53 \frac{e}{\text{cm}} \simeq 7.5 \text{ e/bunch}$$

Using 17 cm bunch length instead of 14 cm would increase this number by less than 10%. Once primary electrons reside in the beam pipe they are attracted by the electrical field of the next bunch. Inserting the full range of values given in table 1 into equation 5 one obtains an electrical field of:

$$E_0 \simeq 0.8 - 1.6\ 10^6 \text{ V/m} .$$

In the following $E_0 = 1.1\ 10^6$ V/m will be used which corresponds to the electrical field with $R = 15$ mm and $\sigma_L = 14$ cm.

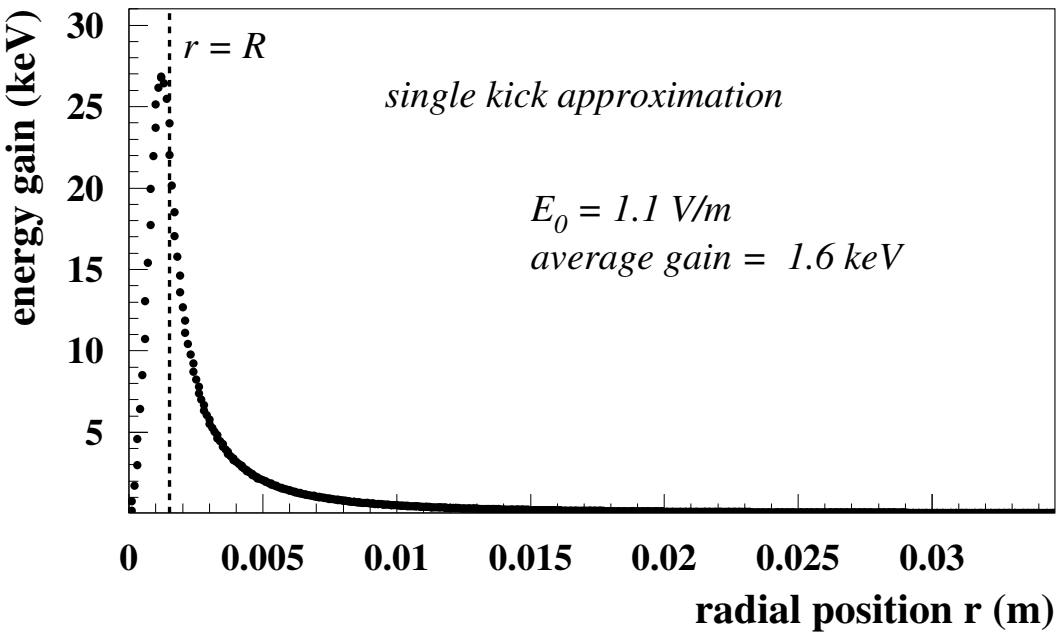

Figure 2: *Energy gain of primary electrons after one bunch passage in the single kick approximation as a function of the radial position in the RHIC vacuum chamber. The dotted line corresponds to the position where r is equal to the radius R of the charge distribution. The average gain corresponds to the mean energy in the range from r=0 cm to r=3.46 cm.*

In the simple model used to estimate a potential electron cloud effect at RHIC, primary electrons are assumed to be stationary. According to [4] this approximation is quite satisfactory and can be applied to electrons with radial positions $r > R$. In the calculations it is assumed that beam gas interactions close to the bunch are more likely. Therefore the assumed density of electrons from gas ionization scales like $1/r$. Figure 2 shows the electron energy after the passage of a bunch in the single kick approximation as a function of its initial radial position. At RHIC an electron residing at the wall at the time a bunch passes by receives an energy of about 40 eV while an electron created closer to the center of the beam pipe may gain several keV up to 25 keV. The mean energy gain for this approximation assuming a medium electrical field of 1.2 10^6 V/m is 1.6 keV.

However, in this approximation the longitudinal bunch shape is not taken into account leading to an overestimation of the energy gained by particles at small radii [13]. Particles which are close to a relatively long bunch are attracted more than once by the electrical field during the passage of the bunch. Therefore such particles perform some oscillations around the center position being accelerated and backtracked again resulting in a significant reduction of the total energy gain. To consider this effect the mean energy gain has been varied from 800 eV to 1600 eV to evaluate the secondary electron yield of the primary electrons.

3.1 Emission Yield of Primary Electrons

If a primary electron gains sufficient energy it crosses the beam pipe and creates secondary electrons in the opposite chamber wall before the next bunch arrives. According to equation 9 the number of released secondary electrons increases with the energy and the angle of incidence with a minimum at normal incidence, $\Theta = 0^o$. Figure 3 shows the secondary electron yield as a function of incoming electron energy for one particular choice of δ_{max} and E_{max}. For each energy setting the angle of incidence has been varied from 0 to 60 degrees. The data points correspond to the average yield while the error bars correspond to the sigma of the variation within the range of 0 to 60 degree in each bin. In this particular case, at a primary electron energy of 1.6 keV, $E_{max} = 300$ V, and $\delta_{max} = 2.0$ the average secondary electron yield δ_1 is about 1.5 for stainless steel. According to [6], the value of δ_{max} differs for stainless steel at 4K (≤ 2) and at room temperature (≤ 1.5). As mentioned before the value quoted in [10] is approximately 1.2 depending on the surface conditions. Therefore the value of δ_{max} has been varied between 1.2 and 2.0 in a range of 300 V $\leq E_{max} \leq$ 500 V. Furthermore the primary energies were changed between 800 eV and 1600 eV as mentioned above. This results in an average secondary

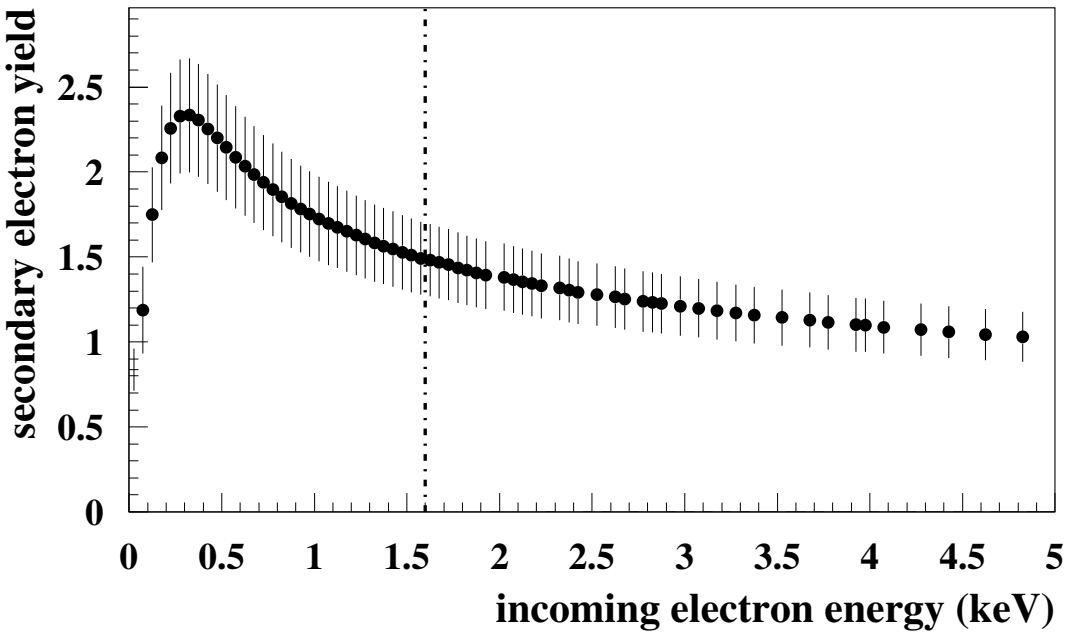

Figure 3: *The secondary electron yield of stainless steel with $\delta_{max} = 2$ and $E_{max} = 300$ eV as a function of the incoming electron energy. The dashed line denotes the average energy gain of the primary electrons.*

electron yield δ_1 for the first generation of:

$$\delta_1 = 1.51 \pm 0.08 \ , \tag{10}$$

where the error corresponds to the error of the mean. In the later calculations of this report the following values have been used as the default:

$$E_{max} = 400\text{V} \ , \tag{11}$$

$$\delta_{max} = 1.8 \ , \tag{12}$$

representing still conservative assumptions. The corresponding value of δ_1 for this parameter set is 1.47 which agrees fairly well with the average value in equation 10.

3.2 Emission Yield of Secondary Electron Generations

The number of electrons N_1 in the beam pipe right after a bunch passage can be written as:

$$N_1 = N_0 \cdot \delta_1 > N_0 \tag{13}$$

where N_0 is the number of primary electrons. These N_1 electrons are slow since most secondary electrons are emitted with low energies usually in the range of 1-10 eV [9]. However, some electrons have an energy up to and including the primary electron energy where the very high energy electrons are backscattered electrons. The integrated number of electrons at an energy equal to the primary electron energy is fairly small ($\mathcal{O}(1\%)$) [9, 14]. Therefore the backscattered electrons will be neglected to calculate the total number of electrons present in the beam pipe just before the next bunch arrives.

The spectrum of the emitted low energy electrons can be approximated by a Maxwell distribution with a maximum value of 10 eV [8] as shown in figure 4 (reflected electrons are not included). The mean secondary electron energy is about 29 eV. Inserting this value in equation 9 results in an average secondary emission yield for the first generation of low energy electrons of $\delta_2 = 0.37$. In the computation the yields are integrated over the effective (i.e. 0-60 degrees) range of angles of incidence (compare figure 3). Table 2 lists emission yields for various energies of incoming electrons. In principle, the spectrum of the low energy electrons is independent of the

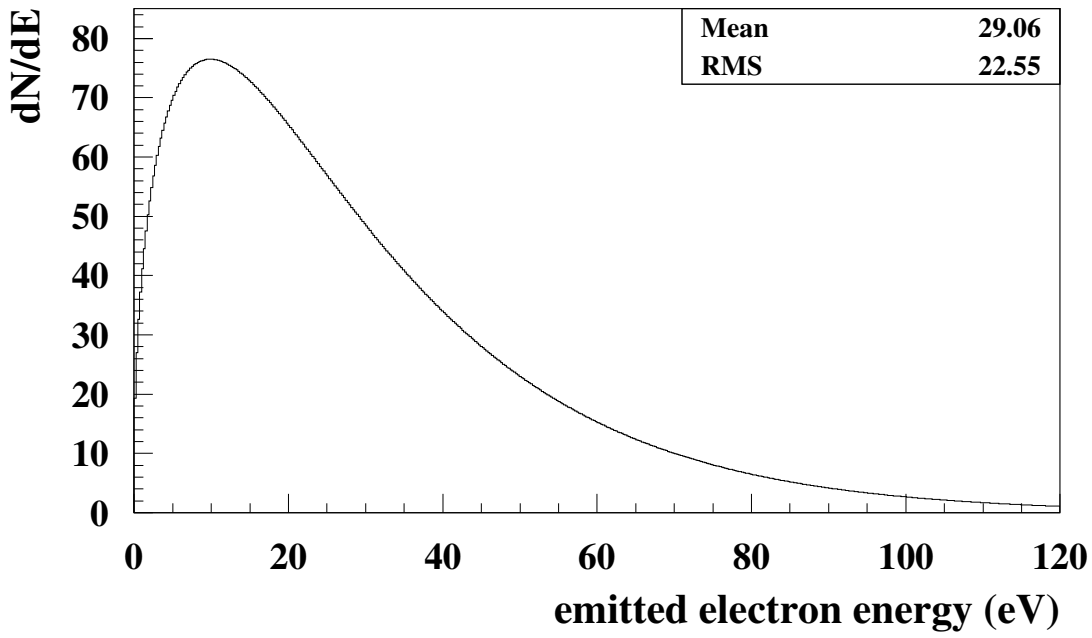

Figure 4: *Low energy spectrum of secondary electron emission for 120 eV incoming electrons.*

energy of the incoming particles and the Maxwell distribution shown in figure 4 can

be applied to secondary electron emission caused by low energy electrons on their part. While in [15] a slightly different approach is used to compute the secondary electron spectrum, the resulting mean energies agree to better than 3% in the two approaches.

In the case of low energies and the Maxwell approach the spectrum is truncated at a certain cut-off value provided this value is still above the maximum value of 10 eV. Depending on the mean energy of the incoming electrons the new mean secondary electron energy and thus the yield δ_2 is reduced from generation to generation of secondary electrons. Table 2 shows the electron yield δ_2 for three generations

generation	E_{cut} [eV]	mean energy [eV]	δ_2
(1)	120	29.1	0.37
(2)	49	21.0	0.28
(3)	34	16.3	0.21

Table 2: *Cut-off energy of the truncated Maxwell distribution, mean energy and secondary electron yield for three generations of low energy electrons.*

and mean energies of incoming slow electrons. The energy of the incoming electrons corresponds to the mean energy of a truncated Maxwell distribution. The cut-off value for the Maxwell distribution in one generation was set to:

$$E_{cut}^{(n)} = E_{mean}^{(n-1)} + E_{RMS}^{(n-1)}, \tag{14}$$

where (n) corresponds to the generation number. The value of 120 eV for the first generation is chosen arbitrarily. Depending on the time gap between two consecutive bunches not only one but several generations of low energy electrons could be created.

3.3 Lifetime of Secondary Electrons in the RHIC Beam Pipe

To calculate the number of electrons $\hat{N}_1$ at the time of the next bunch arrival, the survival probability α in the time gap between two bunches has to be evaluated carefully. α is based on the time of residence of electrons in the vacuum chamber without being absorbed. To derive the total number of electrons, the additional electrons created by the low energy electrons have to be taken into account. The creation of more secondary electrons might happen several times before the next bunch arrives.

Since electrons in a magnetic field are constrained to helices around the field lines, the pattern of particle motion at the presence of a dipole field differs from the motion at a location without field. Therefore RHIC was divided into sections with and without bending field to calculate α. Locations with bending field at RHIC add up to about 40% of the circumference leading to a weight of 0.4 and 0.6 respectively for the two sections. Fig. 5 shows a schematic view of electron motion with and without bending field. While in case (a) for small emission angles the distance electrons cover in the beam pipe rises, in case (b) the electrons are constrained to a motion around the vertical field lines with an increase of the number of cycles for small emission angles. However, the typical time of residence in the beam pipe is about the same in both cases. The average lifetime $\bar{\tau}$ of electrons as a function of

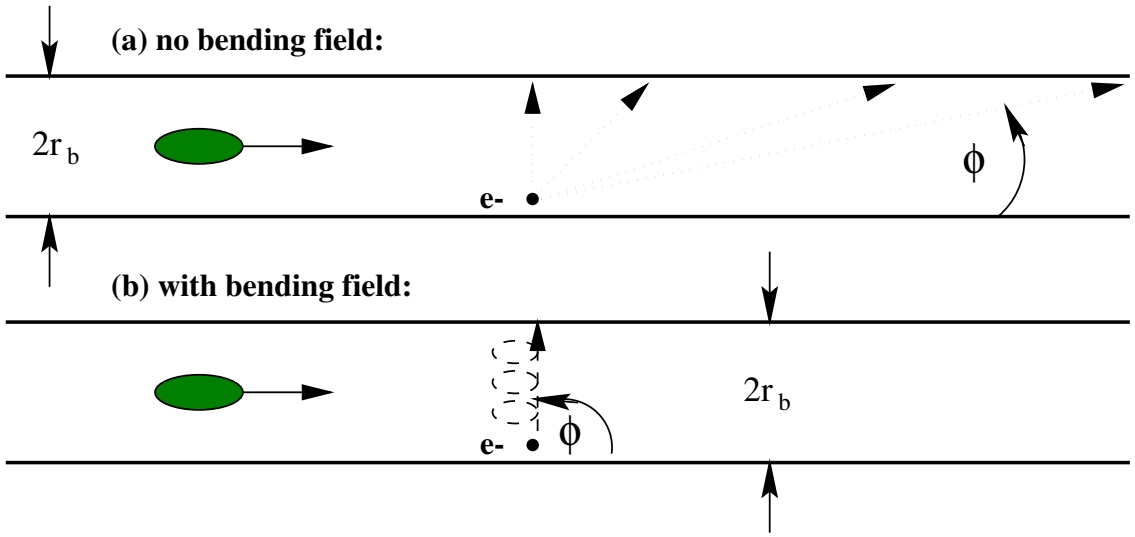

Figure 5: *Schematic view of possible motion of a soft electron emitted from the chamber wall. (a) Location without bending field, (b) location with bending field.*

the emission angle ϕ has been calculated integrating over the entire range of possible emission angles: $0 < \phi \leq \pi/2$, where ϕ is defined as shown in figure 5. Figure 6 shows the crossing time integrated over all emission angles for 29 eV electrons at a location without bending field. No lifetimes below the minimal crossing time, which is in this case about 22 ns, occur. Table 3 summarizes the minimum and mean time of residence in the beam pipe for electrons with energies between 1.6 keV and 21 eV. It demonstrates that at the most 2 generations of slow electrons take place between two consecutive bunches. The survival probabilities are derived from the mean crossing time at the various energies normalized to the spacing time between two bunches, 228 ns and 114 ns respectively and are normalized to the absolute number of electrons which are absorbed at times $t \leq \bar{\tau}$. The survival probability

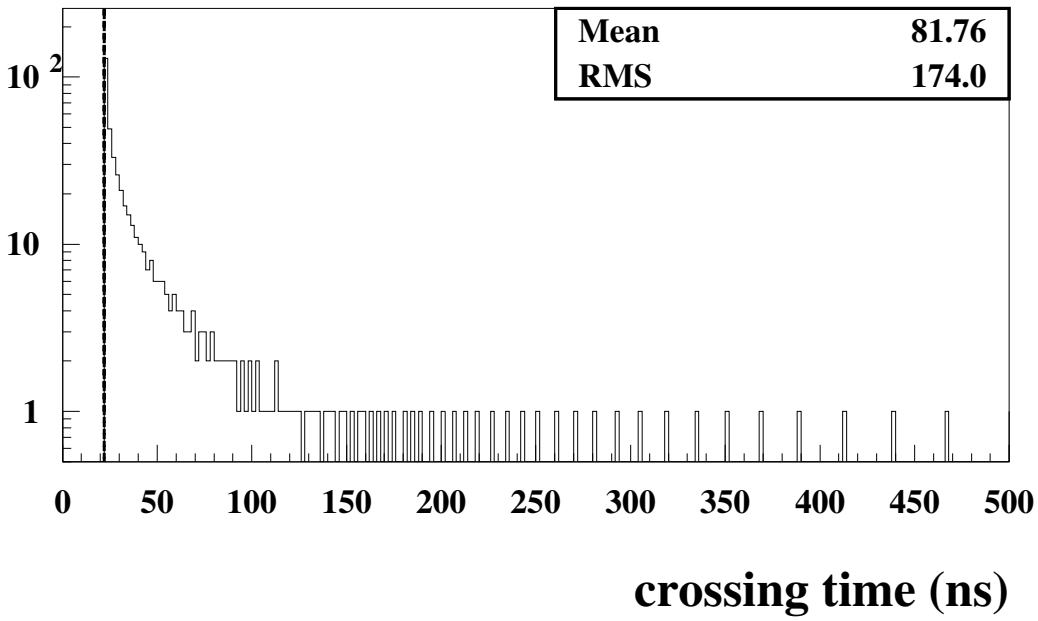

Figure 6: *Lifetime of secondary electrons in the RHIC beam pipe. The energy was set to 29 eV. The mean crossing time is about 82 ns. The distribution is shifted by about 22 ns (indicated by the dashed line) corresponding to the minimal crossing time of an electron with 29 eV and perpendicular emission.*

increases with the reduction of the energy of incoming electrons and the vanishing time gap which remains between the two generations. In the case of a 228 ns time gap a survival probability of 100 % is reached for the second generation. Future potential RHIC upgrades include doubling the number of bunches from 60 to 120 leading to a shortened time gap of 114 ns, where a survival probability of 100 % is met after the first generation already.

On average, the first generation secondary electrons cross the beam pipe within 82 ns at which time they release secondary electrons with a yield of $\delta_2^{(1)} = 0.37$. Given the number of secondary electrons produced by the high energy primary electrons, $N_1 = \delta_1 \cdot N_0$, the number of electrons present at the time the first generation of secondary electrons hit the pipe wall becomes:

$$\hat{N_1}^{(1)} = \alpha^{(1)} \cdot N_1 + (1 - \alpha^{(1)}) \cdot \delta_2^{(1)} \cdot N_1. \tag{15}$$

While $\alpha^{(1)} \cdot N_1$ first generation electrons survive without crossing the beam pipe, $(1 - \alpha^{(1)}) \cdot N_1$ electrons hit the vacuum chamber wall again and either release new secondary electrons with a yield of 0.37 or are absorbed. Using equation 13 an

electron energy [eV]	1600	29.1	21.0
minimal crossing time [ns]	2.9	22	25
mean crossing time $\bar{\tau}$ [ns]	10.8	81.8	94.4
$\bar{\tau}/228$ [ns]	-	0.36	0.64
$\bar{\tau}/114$ [ns]	-	0.7	1.
α (228 ns)	-	0.29	0.54
α (114 ns)	-	0.58	1.

Table 3: *Approximate mean crossing time τ and survival probabilities of electrons in the RHIC beam pipe for various energies.*

effective multiplication factor δ_{eff} can be derived from equation 15:

$$\delta_{eff}^{(1)} = \frac{\hat{N}_1^{(1)}}{N_0} = N_0\delta_1 \cdot (\alpha^{(1)} + (1-\alpha^{(1)})\delta_2^{(1)}) \; . \tag{16}$$

Inserting the numbers listed in table 2 and 3 δ_{eff} is below one for a time gap of 228 ns and above one for 114 ns. The next iteration of Equation15 takes the survival probability $\alpha^{(2)}$ and the emission yield $\delta_2^{(2)}$ of the second generation of slow electrons into account. Thus equation 16 becomes:

$$\delta_{eff}^{(2)} = \frac{\hat{N}_1^{(2)}}{N_0} = N_1 \left(\alpha^{(1)} + \alpha^{(2)}(1-\alpha^{(1)})\delta_2^{(1)} + (1-\alpha^{(2)})\delta_2^{(2)}(1-\alpha^{(1)})\delta_2^{(1)}\right) \; . \tag{17}$$

Further iterations could be evaluated accordingly. Table 4 lists the resulting δ_{eff} for two electron generations. For a time gap of 228 ns two generations are created before the next bunch arrives reducing the "raw" effective yield from 1.47 to 0.70 ± 0.04. For a time gap of 114 ns only one electron generation evolves leading to a saturated effective yield of 1.10 ± 0.07. According to the above approximations, no electron

	(a)	(b)
$\delta_{eff}^{(0)}$	1.47	1.47
$\delta_{eff}^{(1)}$	0.83	1.10
$\delta_{eff}^{(2)}$	0.70	1.10

Table 4: *Effective electron yield as a function of electron generations for (a) a time gap of 228 ns and (b) a time gap of 114 ns. Generation 0 corresponds to the primary electron generation with high energies.*

cloud would appear when RHIC is operated with 60 bunches. However, for the upgraded operation scenario with 120 bunches, an effective yield above 1 remains leading to a probable development of a stable electron cloud in the beam pipe.

4 Discussion of the Results

Taking the results from Table 4, the number of electrons in the beam pipe accumulates in the case of a 114 ns time gap. Within one turn a total of 112 bunches pass followed by 8 empty buckets [16] leading to an enlarged time gap of $8 \cdot 114 = 912$ ns. The time gap corresponds to a length of approximately $l_{gap} \simeq 270$ m. The total number of accumulated electrons, N_e, immediately after the passage of M bunches is given by:

$$N_e = 1.5 \cdot N_0 \cdot \sum_{i=0}^{M-2} \delta_{eff}^{i} \qquad . \tag{18}$$

For $M = 120$ bunches and an effective yield of 1.10 this number amounts to $N_e = 1.3 \cdot 10^8$ while for $M = 60$ and $\delta_{eff} = 0.70$ the number of accumulated electrons is negligible small. The survival probability of these slow electrons during the enlarged time gap is smaller than 8 %. Thus all electrons in the beam pipe get lost during this large gap. However, the absorption process potentially produces a serious heat load in the chamber wall. The integrated dissipated power P, which is deposited in the chamber wall during one entire revolution, is given by:

$$< P >=< E > \cdot \frac{\sum_{i=1}^{M} N_e(i) \cdot e}{t_{rev} \cdot l} \text{ [W/m]}, \tag{19}$$

where l is the length of the interaction area with the pipe wall, $t_{rev} = 12.8\mu$s the revolution time, and $< E >= 1.6$ keV. The total number of electrons, $N_e(i)$, varies according to the number of bunches which come along. The sum over the total number of electrons is the quantity which matters for the integrated dissipated power during one revolution. Inserting the numbers given in the text above leads to $< P >_{60} \simeq 0.3 \cdot 10^{-6}$ W/m with a negligible error and $< P >_{120} = 0.02$ W/m respectively. In the latter case, the effect of even small variations of δ_{eff} is very large due to the sum with the maximum power of δ_{eff}^{M}. Therefore an effective yield of $\delta_{eff} = 1.167$ which corresponds to an upper limit within the error bars as in equation 10 results in a dissipated power of $< P >_{120} = 3.7$ W/m. This is more than two orders of magnitude above the central value.

5 Conclusion

Since the maximum tenable heat load at RHIC is 0.5 W/m [17] the dissipated power of 0.3 mW/m for an operation with 60 bunches is absolutely negligible. Thus we do not expect any problem from beam induced electron clouds for these conditions.

In the case of the upgraded scenario with 120 rotating bunches the number of electrons just after the passage of the 120th bunch is in the order of 10^8 leading to a heat load which is still acceptable. However, even a small addition of +0.07 to the effective yield leads to a power dissipation in the chamber wall of the order of some W/m. This result is 7 times larger than the tenable heat load.

New measurements at CERN [18] indicate that the typical energy of the emitted slow electrons is smaller by about one order of magnitude compared to the approximation of a truncated Maxwell distribution. In such a case where the effective secondary electron yield is practically zero ($\delta_{eff} \simeq 0.04$) all released low energy electrons would be absorbed in the time gap between two bunches without a significant electron accumulation. In addition, recently at LBL evaluated preliminary results from simulations [19] point out a much less severe accumulation effect for RHIC resulting in an inconsiderable heat load even for a 120 bunch operation.

However, within the above discussed simplifications and the error range of the secondary electron yield the heat load exceeds easily the maximum tenable value. Therefore chamber wall overheating is possible for RHIC operation with 120 bunches under the conditions outlined in this report.

6 Acknowledgments

I like to thank a bunch of people who helped in evaluating the electron cloud effect for RHIC with many useful discussions and comments. Among these people are in particular Oliver Brüning, CERN, Miguel Furman, LBL, Dick Hseuh, BNL and Dejan Trbojevic, BNL. Beyond it, special thanks go to Miguel Furman, who applied parts of his simulation code and to Dejan Trbojevic who was available for many long lasting discussions at any time.

References

[1] R. E. Simon and B. F. Williams, "Secondary-Electron Emission", IEEE Trans.Nucl.Sci. NS15 (1968), p. 166 ff.

[2] O. Gröbner, "Bunch Induced Multipactoring", CERN-ISR-VA/77-38 (1977).

[3] F. Zimmermann, "A Simulation Study of Electron-Cloud Instability and Beam-Induced Multipacting in the LHC", LHC Project Report 95 (1997).

[4] O. Gröbner, "Beam Induced Multipacting", LHC Project Report 127, presented at 1997 PAC, Vancouver (1997).

[5] O. Brüning, "Simulations for the Beam-Induced Electron Cloud in the LHC Liner", LHC Project Note 102 (1997).

[6] D. Hseuh, private communication.

[7] Proceedings of CERN Accelerator School, Vol. I, p.269 f, Gif-sur-Yvette, Paris, September 1984.

[8] D. Trines, "The HERA Cold Bore Vacuum system", DESY HERA 85-22 (1985).

[9] N. Rey Whetten in G. H. Haas, Methods of Experimental Physics Vol 4-A.

[10] D. Ruzic et al., " Secondary Electron Yields of Carbon-Coated and polished Stainless Steel", Vac. Sci. Technol., 20(4), April 1982.

[11] RHIC Design Report, August 1992 - September 1995.

[12] J. Wei et al., "RHIC Longitudinal Parameter Revision", RHIC/AP/145 (1997).

[13] S. Berg, "Energy Gain in an Electron Cloud During the Passage of a Bunch", LHC Project Note 97 (1997).

[14] D. Trbojevic, "Heavy Ion Induced Auger Electron, X-Ray, and Optical Emission from a Solid State Surface", Ph.D. Thesis, Goergetown University (1984);
D. Trbojevic, private communication (1997).

[15] M. A. Furman and G. R. Lambertson, "The Electron-Cloud Instability in the Arcs of the PEP-II Positron Ring", LBNL-41123/CBP Note-246/ PEP-II AP Note AP 97.27 (1997).

[16] W. W. MacKay, private communication (1997).

[17] S. Peggs, "Vacuum Pipe Heating in RHIC", RHIC/AP/46 (1994).

[18] I. Collins, LHC division at CERN, private communication 1998.

[19] Miguel Furman, LBL, private communication, March 1998.